Presentation at the National Society of Aerospace Material and Process Engineers Spring Symposium on Space Power Systems Materials, Philadelphia, Pennsylvania, June 3-5, 1963

PROBLEMS OF POROUS TUNGSTEN IONIZERS FOR CESIUM ELECTRIC PROPULSION SYSTEMS

By Albert E. Anglin, Jr. [1963]
National Aeronautics and Space Administration
Lewis Research Center
Cleveland 35, Ohio

ABSTRACT

One of the major metallurgical problems associated with cesium contact ionization for electric propulsion systems is the porous tungsten ionizer. Results of both theoretical and actual sintering studies indicate that tungsten sintering is a grain boundary diffusion mechanism. Under this system, stability and life as an ionizer is less than required for space applications.

Present areas of development for porous tungsten ionizers include studies to overcome these problems as well as the future trends designed to modify or change the sintering process.

I Introduction

Porous tungsten ionizers are a critical problem area in the development of cesium contact ionization thrustors for space propulsion systems. Electric propulsion, as exemplified by a contact ionization source has several potentials for future space missions. These include station keeping, instrumented probes to other planets of the solar system, lunar ferries, and also manned planetary missions. (Refs. 1, 2)

An electric space thrusting unit will consist of an electric power generating source, an electric conditioning system, propellant storage and

feed system and the thrustor device. A mission feasibility comparison of electric systems with other space propulsion systems was recently performed by Spencer et al at JPL. (Ref. 3) Gross payload estimates for 15 missions of interest for a chemical, a nuclear and an electric system are shown in Figure 1, taken from reference 3. The "no mission" designation indicates that the system is incapable of delivering sufficient weight to the required destination or that the delivered gross weight was less than 2000 pounds for the chemical system, and 1500 pounds for the nuclear or electric system. The total transit line in days for each system is also included. All of these missions can be performed with the electric system, while 40% to 50% cannot be performed by the other two systems.

The specific impulse (or the time in which an engine delivers one pound of thrust per pound of fuel) is in the range of 300-350 seconds for the chemical system, 800-1000 seconds for the solid core nuclear system, and 1000-10,000 seconds for the electric system. For electric propulsion systems, which are power-limited, thrust is inversely proportional to the specific impulse, so that the higher the specific impulse, the smaller the thrust and the longer the flight time. Conversely, an increase in specific impulse decreases propellant consumption and increases payload for a given vehicle weight, so that time can be traded for payload weight. Notice that longer transit times are required for the electric system as shown in Figure 1. The exact choice of system for any particular mission, of course, depends on many factors such as cost, availability, reliability, and required trajectory and flight time.

Figure 2 depicts a contact ionization engine. Here cesium is vaporized in a boiler and passes through the thin plates of sintered porous tungsten. When in contact with the tungsten, the cesium atom loses its outer electron

by becoming trapped in the lattice structure of the tungsten. The positively charged cesium ion is then evaporated off the downstream surface of the tungsten ioniser into an electrostatic field created by the electrodes, which accelerates the ions to velocities in the order of 10^5 meters/sec. This velocity is approximately 25 times greater than that from a chemical rocket, and because thrust is proportional to mass flow rate times particle exhaust velocity, the amount or mass of the propellant required for electric rockets is many times less than required by a chemical rocket.

Finally, the electron stripped from the cesium propellant at the ioniser surface is injected back into the ion beam after it leaves the accelerator to prevent a build up of a space charged cloud that essentially would cause loss of thrust.

There are many desirable structural characteristics required for a good ioniser. Besides the necessary strength, corrosion resistance and high temperature properties, we must also include properties which affect the ionization process.

1. High purity, since most impurities can adversely affect the surface work function.

2. Pore size, since large pores cause a large amount of neutral atoms to be emitted. These neutral atoms can be ionized by charge exchange inside the ion accelerator. When this occurs, the resulting ions will fall into the accelerating electrode and cause sputtering, thus lowering engine life. The pore size in the tungsten emitter should be approximately one micron or less in diameter.

3. Pore spacing, since large spacing results in low current density. A low current density results in increased engine frontal area and reduced

power efficiency. Hussmann (Ref. 4) considers proper spacing to be 10^7 pores per square centimeter, so that approximately two or three microns separate each pore.

4. Stability, since for long duration missions over 10,000 hours of operation is required. Any change in the ionizer cannot be tolerated, so that stringent requirements are placed on the porous tungsten. At present, all the requirements have yet to be satisfied by powder metallurgical techniques.

Attempts to achieve the proper purity, pore size, and spacing have apparently been realized by eleutriation and spheroidization techniques. High purity hydrogen reduced tungsten powder of certain particle size distribution is first plasma sprayed in inert gas to produce the spherical particles. The resultant wide distribution of particles are then eleutriated by air or other techniques to produce the one to three micron particles desired.

Spherical particles are considered capable of being compacted and sintered to a high uniform density; however, the hardness of the tungsten spheroids makes compacting pressures over 50,000 psi necessary, and the green strength and handling ability is poor. Sintering characteristics to date on these compacts are inconclusive, and there is no data on their ionizing properties. Unfortunately, the results available on sintering of both hydrogen reduced and preliminary data on spherical tungsten powders indicate a major problem area exists.

In this paper we will first discuss the results obtained in the sintering of hydrogen reduced tungsten powder, varying temperature, time, and particle size on hydrostatically pressed powders.

Second, we will discuss the sintering theory as outlined by Kuczynski, demonstrating that its simplified approach must include first a grain

boundary and volume diffusion mechanism and, second, an evaluation of the neck width by considering various packing systems.

Third, by the use of these two major modifications, we will calculate sintering rates based on both grain boundary and volume diffusion mechanisms. We then will demonstrate that the experimental data fit the grain boundary diffusion model. Using the considerations of Jordan and Duwez, we shall show that any grain boundary diffusion mechanism is unstable, because densification actually continues through the first 100 hours. Experimental and theoretical data indicate that long life is doubtful for ionizer applications with porous tungsten without modification.

Finally, we shall show that only by volume diffusion is ionizer stability insured and discuss some of the methods by which this mechanism can be obtained.

II Results of Sintering Hydrogen Reduced Tungsten Powder

At the Lewis Research Center unpublished experimental data have been obtained by N. Saunders and T. Reynolds on the sintering rates of hydrogen reduced tungsten powder of irregular shape. They used two average particle size ranges of 1.1 and 0.88 microns and these were hydrostatically pressed at 25,000 psi and sintered at temperatures from 1430° - 1660° C. This data together with the results of a sintering study carried out by Gerken, Hiltz and Lally (Ref. 5) of TAPCO are shown in Figure 3 depicting the change in percent of theoretical density against sintering time plotted on a log-log basis. All powders were hydrostatically pressed at 25,000 psi and sintered in a hydrogen atmosphere. Although the data were obtained from two sources, excellent agreement is shown between laboratories for one micron particles of hydrogen reduced powder. The method of plotting demonstrates a straight line relationship between sintering temperature and densification up to 100 hours.

Accompanying the temperature-densification rate of one micron particles is Figure 3A depicting the effect of particle size on density for a sintering temperature of 1930° C. All powders were presintered at 1230° C for 6 hours before the high temperature final sinter. All results for this figure were obtained at TAPCO. Further experimental results have been obtained by R. Turk at the Hughes Research Laboratories (Ref. 6) for hydrogen reduced tungsten powders. Turk's results are shown in Figure 3B which depicts the change in density of two particle sizes (0.5-1 microns and 3-3.5 microns) at two sintering temperatures (1500° and 1600° C) for times to 100 hours. The resulting straight lines as plotted have been extended to 1000 hours. The density slope versus time is comparable to the other investigations (Figure 3 and 3A) within the limitations imposed by differences in particle size, shape, distributions, compact pressure, and sintering temperatures.

None of the figures show the green compacting density starting from a zero time. These curves originate after either a pre-sintering period of 1-6 hours at approximately 1200° C, or allowance is made essentially for both the compact and furnace to reach stabilizing conditions.

III Sintering Theory

G. C. Kuczynski has demonstrated the usefulness of applying his theoretical approach of sintering to practical results. (Refs. 7, 8, 9, 10) This application is generally demonstrated on direct measurement of sintered wires where the neck width between the spherical cross section grows at a rate commensurate with either a surface effect or a diffusion mechanism. In this paper in application of his theory to sintering of tungsten powders, we will only utilize that portion of Kuczynski's theory dealing with the diffusion mechanism. Kuczynski accounts for two mechanisms, either by

surface or volume diffusion. Although he mentions grain boundary diffusion, he does not differentiate between volume or grain boundary diffusion. He further so simplifies his sintering model that unless the neck growth can be measured visually, it is difficult to apply his theory to regular sintering systems. A short review of Kuczynski's models is in order so that application can be made to practical sintering systems.

The prime consideration of Kuczynski's theory lies in the relationship of $\frac{X}{a}$ where "X" is the neck width and "a" is the particle radius. (Figure 4) He considers sintering a two-stage process. The first stage considers growth of the neck X without any decrease in center to center distance of the particles. The second stage shows a further increase in the neck width X accompanied by a decrease in inter-particle distance (actual shrinkage).

In order for us to apply his theory, we first must consider the relationship between several particles in a complex system and the methods of packing in this system. This spherical packing has been considered by V. T. Morgan in detail. (Ref. 11) He demonstrates two basic methods of packing whereby all other systems can be considered modifications of these two. These two basic types are shown in Figure 5 and consist of rhombic (close packed) and cubic (open) packing. Morgan demonstrates that by stacking layers of either of these two systems one on top of the other, various combinations are possible. However, it is beyond the scope of this paper to detail his models. In consideration of his two basic types, both the pore area and particle contacts are quite dissimilar, and we can expect sintering effects to be quite different. Morgan pictorially explains the various packing systems in detail in his paper. (Ref. 11)

Duckworth, in work with copper and lead spheres, has measured the open volumes between the spheres during sintering and also the angle of contact

formed to full densification. (Ref. 12) He found that the area of contact between spheres of equal diameters increases as the angle ϕ increases and depicts a different angle for each basic type of packing. Duckworth's results can be clarified by further consideration of Figure 5. Duckworth measured the angle ϕ between two adjacent particles, as shown, and he found the area of the contact between two equal particles varied as

$$\pi r^2 \sin^2 \tfrac{1}{2}\phi \qquad (1)$$

When the spheres just touch each other, he considers the angle ϕ equal to zero, while the space between particles is equal to the hatched area as shown in Figure 5. The space available decreases as the contact angle increases until, at full density, the angle formed in rhombic packing equals 60 degrees, while cubic packing ϕ equals 90 degrees. Considering in three dimensions the two basic structures, they are then taken by Duckworth into the various packing systems. The results of these two structures are shown in Figure 6, together with two other systems of packing. Here he depicts porosity (volume available), as equivalent density vs. contact angle for the four systems.

Considering Duckworth's systems in relation to the packing of tungsten spherical powder, we note from Figures 3A and 3B that by hydrostatic packing, approximately 60% density is attained. For our considerations, we will use this packing density to utilize Duckworth's measurements since tungsten itself has a body centered cubic packing system the same as the orthorhombic packing. Note that the orthorhombic system can attain a 60.5% original packed density.

In order to interrelate Duckworth's models with Kuczynski's, we need first establish the relation of the angle, the neck width, and the orthorhombic

packing system. Basically, Duckworth considers the angle ϕ being zero at the start where only interparticle contact is established. If we consider a simple cubic packing system, as shown in Figure 7, then θ in this model will also equal zero when the spheres are first touching. As the neck width X grows, θ will increase. However, when Duckworth's angle ϕ shows 90 degrees at full density, for our considerations, the angle formed can only be $\frac{\theta}{2}$ or 45 degrees. Therefore, the neck width can only increase between zero and 45 degrees and the width increase as

$$X = a \, TAN \frac{\theta}{2} \qquad (2)$$

where "a" equals the radius.

A problem presents itself in accounting for shrinkage, i.e., a decrease in center to center distance between particles, whereby both radii are decreasing while angle θ is increasing. We can eliminate this problem by two considerations, the first being that the material for the neck width comes from the area between particles by a grain boundary diffusion mechanism, as under Kuczynski's theory and, second, that his next step will be by volume diffusion of atoms into the vacancy (void). We, therefore, will have a two-rate system, the slower second (volume diffusion) taking place when the angle θ exceeds 30 degrees. In orthorhombic packing this is equivalent to 81% density and is assumed to be the maximum angle formed where the variation between the angle and porosity becomes linear.

Under these two considerations, if we assume that the neck width X distance proceeds to fall on an arc formed by the original surface of the sphere, then both considerations will be satisfied at both 100% density and at 60.5% density. This allows both shrinkage (densification) and neck

growth to proceed together. The neck width then, by proceeding along an arc, will vary as

$$X = \frac{2\pi\,\theta\,a}{360\;2} \tag{3}$$

We have calculated the neck width and included angle $\frac{\theta}{2}$ as a function of density by both methods in Tables I and II for particle diameters from 0.5 to 5.0 microns. The tables show the variation of porosity and density as θ increases. From zero to 30 degrees, the neck width can be considered equivalent by both methods. Above 30 degrees, however, the systems show deviation whereby the neck width at 100% density for the straight line method is 21% less than that for the arc method.

We will use the arc method for our calculations using Kuczynski's basic theory. The comparison of particle diameter and neck width X vs. angle θ with density are shown in Figure 7A.

Kuczynski has two formulas for calculating diffusion sintering:

1. Surface diffusion

$$\frac{X^7}{a^3} = \frac{56\,\gamma\,V_0\,D_s\,t}{KT} \tag{4}$$

2. Volume diffusion

$$\frac{X^5}{a^2} = \frac{100\,\gamma\,\delta^3\,D_v\,t}{KT} \tag{5}$$

He considers grain boundary diffusion to be a part of volume diffusion. However, Langmuir (Ref. 13) and Le Claire (Ref. 14) determined that for diffusion of thorium in tungsten, there are three diffusion mechanisms. Their results are plotted in Figure 7B, where the log of the diffusion rate D is plotted against the reciprocal of temperature, resulting in straight lines.

They determined that the slope of these lines is equal to the energy of activation of the system Q, where the diffusion rates are given by

$$D = D_0 e^{-\frac{\theta}{RT}} \qquad (6)$$

In our consideration of the sintering of tungsten, we have not considered sintering by a surface diffusion mechanism, not only because of its rapid sintering rate, but also we are dealing essentially with self-diffusion of the tungsten atoms without impurity additions such as thorium as shown in the graph.

IV Calculation of Neck Width, Density and Pore Volume with Kuczynski's Theory

Kuczynski's volume diffusion formula

$$X^5 = \frac{100\gamma\delta^3 a^2 D_v t}{KT} \qquad (7)$$

so that rearranging his volume diffusion yields:

$$5 \log X = \log t + \log\left(\frac{100\gamma\delta^3 a^2 D_v}{KT}\right) \qquad (8)$$

We can show the increase of X (neck width) with time for a particle diameter at a given temperature. For example, for a 2 micron diameter particle at 2000° K, for volume diffusion, ($D = 2.303 \times 10^{-13}$ cm^2/sec).

Time	X(microns)	Density From Fig. 4
1 hr.	0.034	61.0%
10 hrs.	0.053	61.5%
100 hrs.	0.094	62.5%
1,000 hrs.	0.135	64.0%
10,000 hrs.	0.213	67.0%

By comparison with Table II or Figure 4, we see that the density increased in 10,000 hours approximately 6%.

For grain boundary diffusion, we have utilized the same formula of Kuczynski except D_{GB} is substituted for D_V, or volume for grain boundary diffusion, from Figure 5. These theoretical results for both grain boundary and volume diffusion at temperatures of 1125°, 1725°, and 2200° C whereby times up to 10,000 hours are plotted against density in Figure 8.

From these theoretical considerations and from the actual sintering curve as taken from Figure 3B, we can see that the normal tungsten sintering system can be considered to be by a grain boundary diffusion mechanism. To further substantiate this, we have calculated using Kuczynski's method of plotting $\log \frac{x}{a}$ vs. the log of time in hours, for 0.5 micron diameter particles at temperatures of 1152°, 1752°, and 2200° C and plotted these results in Figure 8A. Comparing these rates with Hughes data for 0.5-1.0 micron diameter particles at 1660° C supports a grain boundary diffusion mechanism.

Caution, however, must be taken since none of the data is complete beyond 100 hours. From theoretical considerations, we should see a rate change as previously mentioned at approximately 80% density. This rate change would demonstrate the onset of a volume diffusion mechanism. We have plotted all grain boundary diffusion rates even over 80% density as straight lines (contrary to theory) where they actually should demonstrate a lower rate change to accommodate Morgan's and Duckworth's approach. Essentially, we need further substantiating data before the theoretical approach can be considered accurate. The same sintering data taken to 250 hours, especially for the 0.8 micron diameter particles, should demonstrate this rate change.

A further method of visualizing the relationship between effect of density, time, temperature, and particle size is that of Jordan and Duwez (Ref. 15) where they plot the relation of log time vs. the reciprocal of the

temperature for various values of sigma (σ). An approximate set of straight lines result. They define σ as the relation between theoretical, pressed and sintered density.

$$\sigma = \frac{D_s - D_p}{\rho - D_p} \qquad (9)$$

They point out that one can expect densification to be a simple rate process behaving according to a relation of the type

$$LOG\left(\frac{t_1}{t_2}\right) = \frac{Q}{R}\left(\frac{1}{T_1} - \frac{1}{T_2}\right) \qquad (10)$$

The relations σ , D_s, $D_s - D_p$ and density are shown in Table III.

Figure 9 shows both the Hughes data for 0.5-1.0 microns and theoretical calculations for 1 micron particles plotted in this manner assuming a grain boundary diffusion mechanism (without any rate change to volume diffusion).

Figure 10 shows the theoretical volume diffusion mechanism for 1-2 micron diameter particles, demonstrating but slight densification over 10,000 hours.

The usefulness of this type plot can be shown by first considering Figure 9, which is the actual sintering data. If we consider starting with a 70% density at 1267° C, then the time to proceed to an 80% density can be shown to be (300-100 hours) or 200 hours. Similarly, at 1062° C from 70 to 80% density would take approximately 500 hours.

If we consider the theoretical grain boundary diffusion mechanism for the 1 micron diameter particles in Figure 9, then to again proceed from a 70 to 80% density at 1267° C (100-6) would take 94 hours, while at 1062° C (600-60) the time would be 540 hours.

Under volume diffusion, however, as shown in Figure 10, there would be

no appreciable density increase at either 1267° C or 1062° C for times to at least 10,000 hours.

V Discussion of Results

It has been demonstrated that using a modified Kuczynski approach, sintering of both spherical and hydrogen reduced tungsten powder proceeds according to a grain boundary diffusion mechanism. There is insufficient data to demonstrate whether a volume diffusion mechanism takes place over 80% density. However, it does show that for porous tungsten sintered below 80% density, at temperatures of 1100° - 1300° C further densification will take place, which will certainly affect the properties as a cesium contact ionization source since, basically, an increase in density is accompanied by a decrease in porosity.

Unpublished data by N. T. Saunders and T. W. Reynolds of NASA measured the transmission coefficient using nitrogen as the gas and found that the coefficient decreases rapidly above 85% density for both commercially made and NASA hydrogen sintered porous tungsten plates. Figure 11 depicts part of their data showing that densification affects the transmission coefficient.

The transmission coefficient C as defined is:

$$C = \frac{\text{Mass departure rate}}{\text{Mass arrival rate}} \qquad (11)$$

This figure shows essentially zero permeable porosity over 88% density.

Generally, the transmission coefficient is constant below 10 MM Hg, which is the level generally used for ion propulsion, so that flow can be considered in the free-molecular range through the porous tungsten plug.

Since there is indication of further sintering with time even at ionizing temperatures, any change in transmission coefficient can be shown to affect the current density. (Refs. 4, 16, 17)

If the transmission coefficient is known, the current density effect can be estimated by

$$\mathcal{J}_{CS} = 490C \frac{P_{mm}}{\sqrt{T}} = AMPS/CM^2 \qquad (12)$$

The effect would be to lower not only the current density but also to decrease the diffusion rate of cesium atoms onto the surface of the tungsten.

Accompanying any change in density is shrinkage and, as such, it becomes problematical whether cracking will take place before any system change to volume diffusion rate is possible.

The major consideration then becomes one of attaining volume diffusion by changing or modifying the sintering system. This possibility is feasible along several avenues of approach.

1. Grain boundary removal by essentially reducing the recrystallization temperature of the tungsten. This includes the addition of a second metal chosen so that the surface ionization properties would not change. Essentially, the addition should have solid solubility in tungsten and the amount added would normally be slight, probably less than 1%.

2. Utilizing diffusion rate effects by the addition of a second metal from Group IV of the Periodic Table. Here, the metal (by diffusing more rapidly into tungsten than tungsten into the metal) will, depending on the composition (percent) hopefully stabilize the system. The tantalum-tungsten system has demonstrated not only this diffusion effect but also porosity is at a maximum at approximately equal atomic percentages.

3. Adding an eutectic forming metal which would affect the sintering rate. Again, any additions would, of necessity, be minimum; however, a careful examination of this technique might demonstrate the opposite effect, whereby diffusion sintering might continue as a grain boundary mechanism.

4. Adding dispersed phase hard particle additions which are insoluble in tungsten. Most carbides, nitrides, and oxides appear to have either lower work functions or else they are unknown. (Ref. 18) Lower work function materials may affect ionization but hopefully the hard particles will exist at the grain boundary apex and not affect the ionization process. It must be pointed out, however, the necessity of obtaining 0.1-0.2 micron particles insoluble in tungsten with high work functions and probably existing as nitrates or acetates for simplicity of addition. These become somewhat difficult to find.

5. Liquid phase sintering has possibilities by utilizing the solution or Kirkendahl effect of a soluble metal in a liquid phase carrier. This system shows potential methods of producing stable ionizers that have no press or size limitation, nor is it necessary to use spherical powder, hence, costs would be minimum. It is felt that the desired pore size could ge achieved provided that both the soluble metal and the carrier can be completely removed in a vacuum evaporation technique.

These attempts at modification are, in one form or another, in the process of being experimentally evaluated at several different laboratories. Hopefully, the stability and life of a porous tungsten ionizer will be achieved by these studies.

VI Summary

Comparison has been made between actual sintering rates of tungsten powder in the .5 to 15 micron diameter size range and a theoretical model based on grain boundary diffusion rates. The model was shown to result in similar rates as actually obtained by several investigators. Application of these rates to the porous tungsten structures used as ionizing surfaces

in electric thrusters would indicate that further densification would occur at the temperatures of operation. This further densification was shown to be detrimental to thrustor performance and for required mission times expected in the future could lead to complete clogging of the pores and cessation of thrust. Possible methods were discussed that might be employed to slow these sintering rates to obtain time-temperature stability in an electric thrustor environment.

TABLE I

Calculation of neck width and included angle vs. density by $\text{Tan}\frac{\theta}{2} = \frac{X}{A}$

$X = \text{Tan}\frac{\theta}{2} A$

Angle		Neck Width (microns)(a)				Porosity	Density %
θ	$\frac{\theta}{2}$	0.5 diam.	1.0	2.0	5.0		
0	0	0	0	0	0	0.395	60.5
5	2.5	.0109	.0218	.0436	.109	.388	61.2
10	5	.0219	.0437	.0875	.219	.375	62.5
20	10	.044	.088	.176	.44	.350	65.0
30	15	.067	.134	.278	.67	.320	68.0
40	20	.091	.182	.364	.91	.285	71.5
45	22.5	.107	.207	.414	1.07	.263	73.7
50	25	.1165	.233	.466	1.165	.238	76.2
60	30	.144	.288	.577	1.44	.198	81.2
70	35	.175	.350	.700	1.75	0.15	85.0
80	40	.209	.435	.839	2.1	.065	93.5
85	42.5	.229	.458	.916	2.29	.030	97.0
90	45	.25	.5	1.0	2.5	0	100

TABLE II

Calculation of neck width and included angle vs. density by

$$X = \text{arc} = \frac{2\pi}{360} \times \frac{\theta}{2} = 0.01745 \times \text{radius} \times \frac{\theta}{2}$$

Angle		Neck Width (microns)				Porosity	Density %
θ	$\frac{\theta}{2}$	0.5 diam.	1.0	2.0	5.0		
0	0	0	0	0	0	0.395	60.5
5	2.5	.0109	.0228	.0437	.109	.388	61.2
10	5	.0218	.0436	.0875	.218	.375	62.5
20	10	.0436	.0872	.174	.436	.350	65.0
30	15	.065	.130	.260	.650	.320	68.0
40	20	.0867	.173	.346	.867	.285	71.5
45	22.5	.0982	.196	.392	.982	.263	73.7
50	25.0	.109	.218	.436	1.09	.238	76.2
60	30	.131	.262	.524	1.31	.198	81.2
70	35	.153	.305	.612	1.53	.150	85.0
80	40	.1745	.349	.698	1.745	.065	93.5
85	42.5	.1855	.371	.742	1.855	.030	97.0
90	45	.196	.393	.785	1.96	0	100

TABLE III

Calculation of σ (sigma) from Jordan and Duwez

Tungsten = 19.3 gms/cc density = ρ D_p = 11.8 = 60.5%

$$\sigma = \frac{D_S - D_p}{\rho - D_p} \qquad \rho - D_p = 7.5$$

D_S	$D_S - D_p$ (60%)	σ	Density %
19.3	7.5	1.0	100
19.0	7.2	0.96	98.5
18.5	6.7	0.89	95.8
18.0	6.2	0.83	93.2
17.5	5.7	0.76	90.5
17.0	5.2	0.69	88.0
16.5	4.7	0.67	85.5
16.0	4.2	0.57	83.0
15.5	3.7	0.49	80.3
15.0	3.2	0.43	77.7
14.5	2.7	0.36	75.2
14.0	2.2	0.29	72.5
13.5	1.7	0.23	90.0
13.0	1.2	0.16	67.4
12.5	0.7	0.093	64.7
12.0	0.2	0.026	62.2
11.8	0	0	60.5

APPENDIX - SYMBOLS

a = radius of particle - cm.

A = area of porous medium - cm^2

D_V = volume diffusion coefficient - cm/sec.

D_{GB} = grain boundary diffusion coefficient - cm/sec.

D_o = diffusion constant

D_S = density after sintering - gms/cc.

D_P = density after pressing, before sintering - gms/cc.

δ = interatomic distance - W = 2.7 Å = 2.7×10^{-8} cm.

γ = surface tension of W = 1900 dynes (theoretical)

K = Boltzman's constant - 1.375×10^{-16} ergs/deg. = dynes cm^{-1}

M = molecular weight

P_{MM} = mean absolute pressure of gas in chamber - MM Hg

δP_{MM} = decrement of pressure in δ t seconds - MM Hg

Q = energy of activation = 135,000 K cal for volume diffusion

R = gas constant - 82.056 $\frac{\text{cc atom}}{(^oK)(\text{gm mole})}$ or 8.317×10^7 ergs/mole deg.

T = temperature ^{o} K

t = time - seconds

ρ = density of the solid - gms/cc.

V = volume of gas in test chamber - cm^3

σ = densification constant - dimensionless

θ = angle forming contact between spheres - degrees

X = neck width - cm.

ϕ = angle forming width of neck - degrees

V_o = atomic volume - W = 9.53 cu cm/g - atom

REFERENCES

1. W. R. Mickelsen, "Electric Propulsion for Space Flight," Aerospace Engineering, Vol. 19, No. 11, November, 1960.

2. W. E. Moeckel, "Electric Propulsion for Spacecraft," NASA SP-22, NASA-University Conference on Science and Technology of Space Exploration, Chicago, November, 1962.

3. JPL Technical Report, 32-281, "Nuclear Electric Spacecraft for Unmanned Planetary and Interplanetary Missions."

4. O. K. Husmann, "Comparison of the Contact Ionization of Cesium on Tungsten, etc.," AIAA Electric Propulsion Conference, Colorado Springs, Colorado, March, 1963.

5. "Development and Testing of Tungsten Emitters for Ion Propulsion Systems," TDR No. ASD-TDR-62-756, Wright-Patterson AF Base, Ohio.

6. Hughes Research Laboratories, Summary Progress Report, Contract NAS 5-517, September, 1962.

7. G. C. Kuczynski, Journal of Metals, 1949, Vol. I (2), pp. 169-178.

8. G. C. Kuczynski, Acta Met., 1956, Vol. IV (1), pp. 58-61.

9. G. C. Kuczynski, Journal of Applied Physics, 1949, Vol. XX, pg. 1160.

10. G. C. Kuczynski, Powder Met., ed. W. Leczynski, Interscience, N. Y., 1960.

11. V. T. Morgan, Symposium on Powder Metallurgy, Special Report No. 58, Iron and Steel Inst., 1956, pp. 81-89.

12. W. E. Duckworth, Symposium on Powder Metallurgy, Special Report No. 58, Iron and Steel Inst., 1956, pp. 213-218.

13. I. Langmuir, J. Franklin Inst., Vol. 217 (5), 1934.

14. A. D. Le Claire, Progress in Metal Physics, Vol. I, 1949.

15. C. B. Jordan and P. Duwez, Journal of Metals, 1949, Vol. I (2), pp. 96-99.

16. R. G. Wilson, G. D. Seele and J. F. Hon, "Surface Ionization of Cesium with Porous Tungsten Ionizers," AIAA Electric Propulsion Conference, Colorado Springs, Colorado, March, 1963.

REFERENCES (Continued)

17. T. W. Reynolds and L. W. Kreps, "Gas Flow, Emittance and Ion Current Capabilities of Porous Tungsten," NASA TN D-671.

18. J. H. Affleck, "Investigation of Various Activator-Refractor Substrate Combinations," AF CRC-TN-60-104, SCI REP 1-13, Contract AF 19(604)-4093.

19. Rutledge and Rittner, Journal of Applied Physics, Vol. 28, pg. 167, 1957.

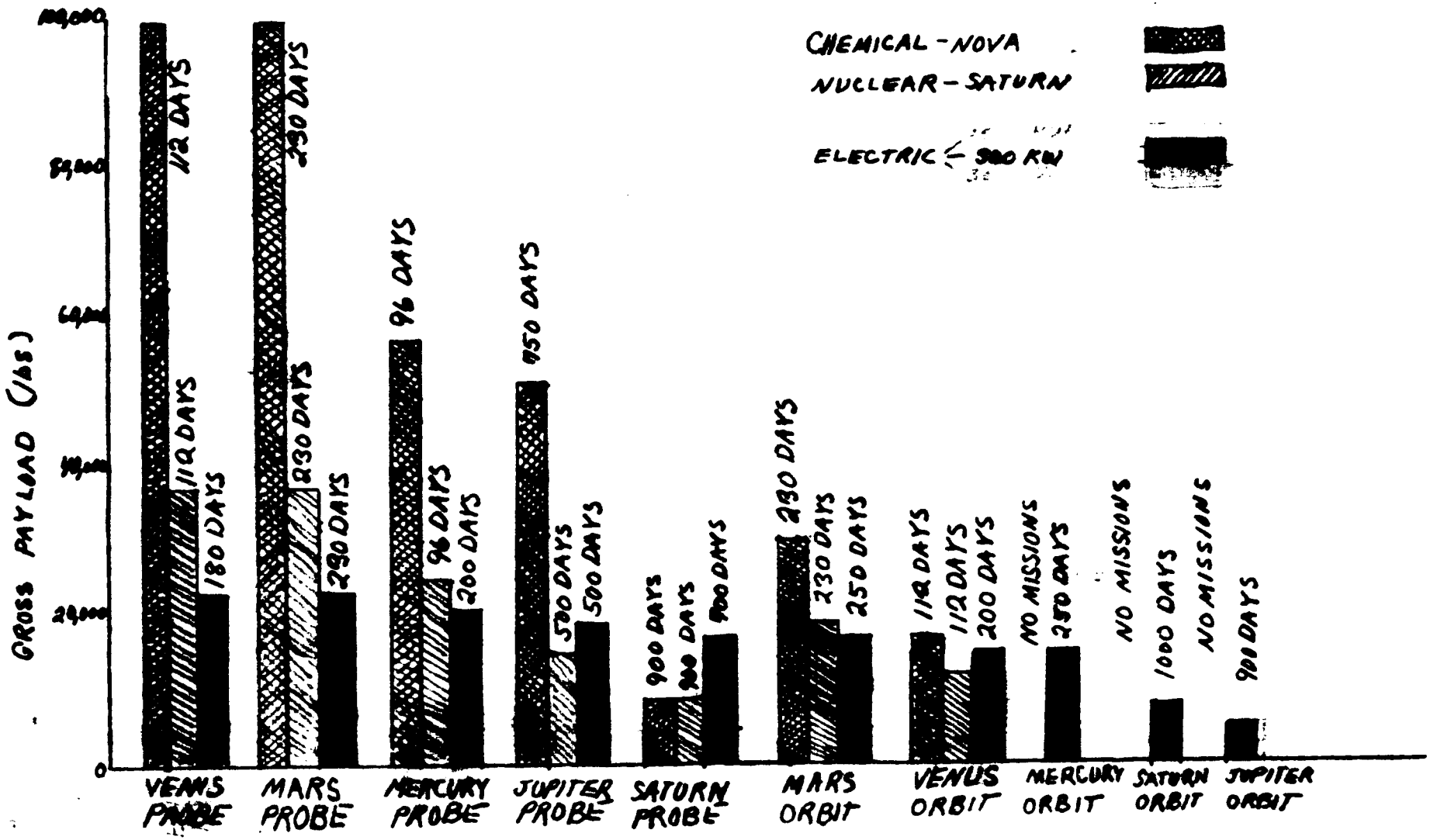

FIG. I. PERFORMANCE COMPARISON OF CHEMICAL, NUCLEAR, AND ELECTRIC SYSTEMS

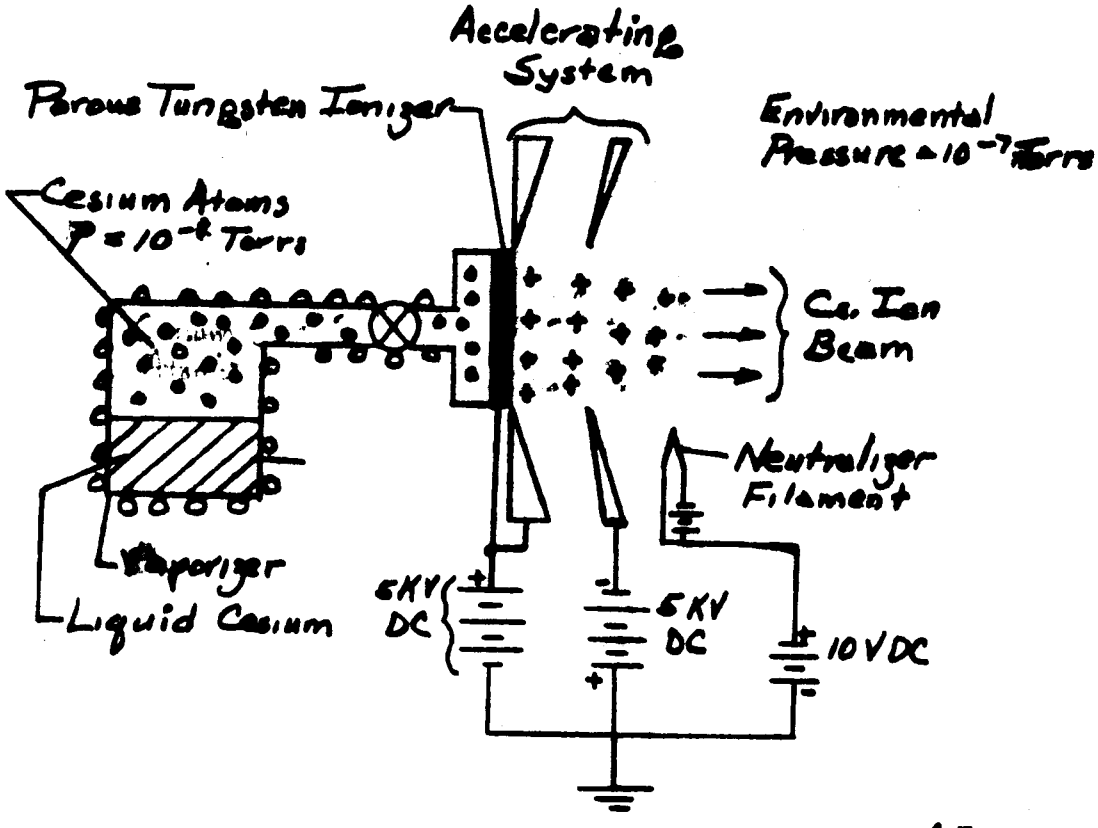

Fig. 2 Schematic of a Cesium Ion Thruster Utilizing Porous Tungsten Ionizers.

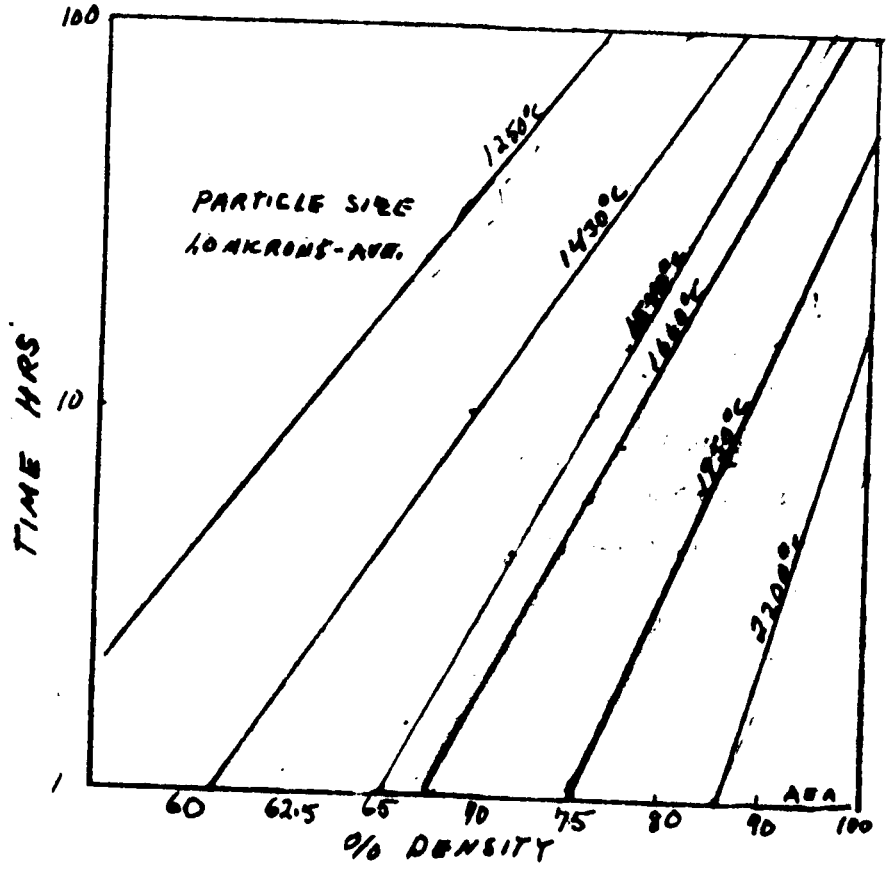

FIG 3 EFFECT OF DENSITY ON SINTERING TIME FOR [redacted]

ATMOSPHERE - HYDROGEN
COMPACTING PRESSURE - 25,000 PSI

E-2130

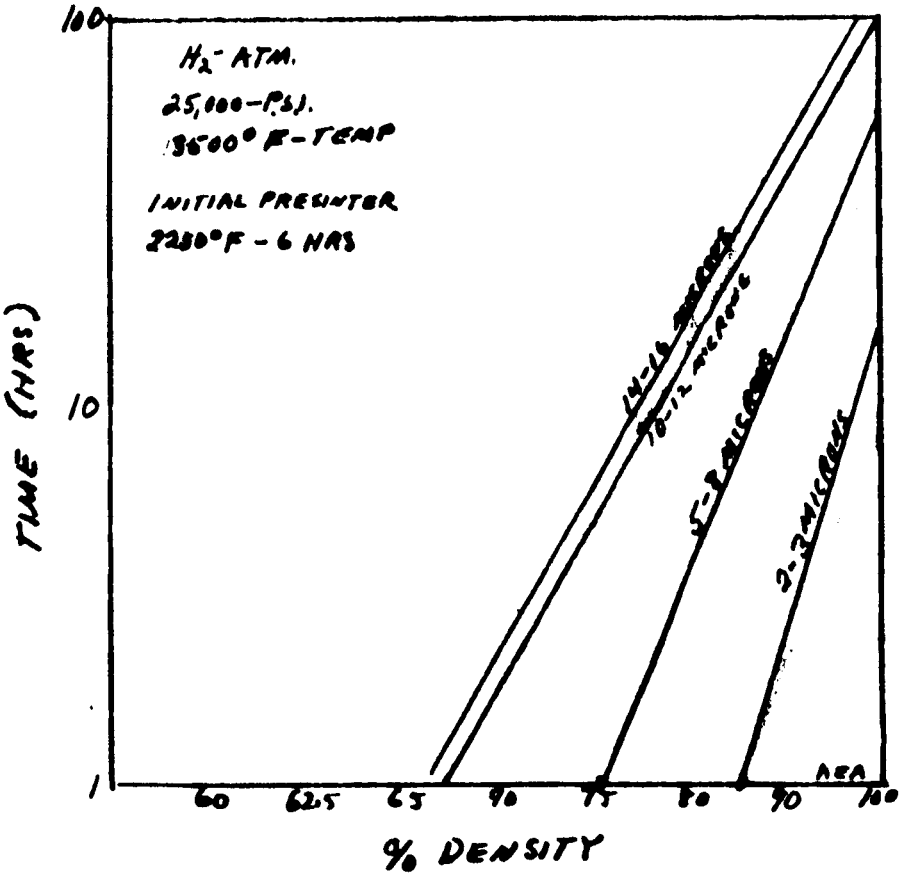

FIG 3A EFFECT OF DENSITY ON SINTERING TIME FOR DIFFERENT PARTICLE SIZES OF TUNGSTEN POWDERS

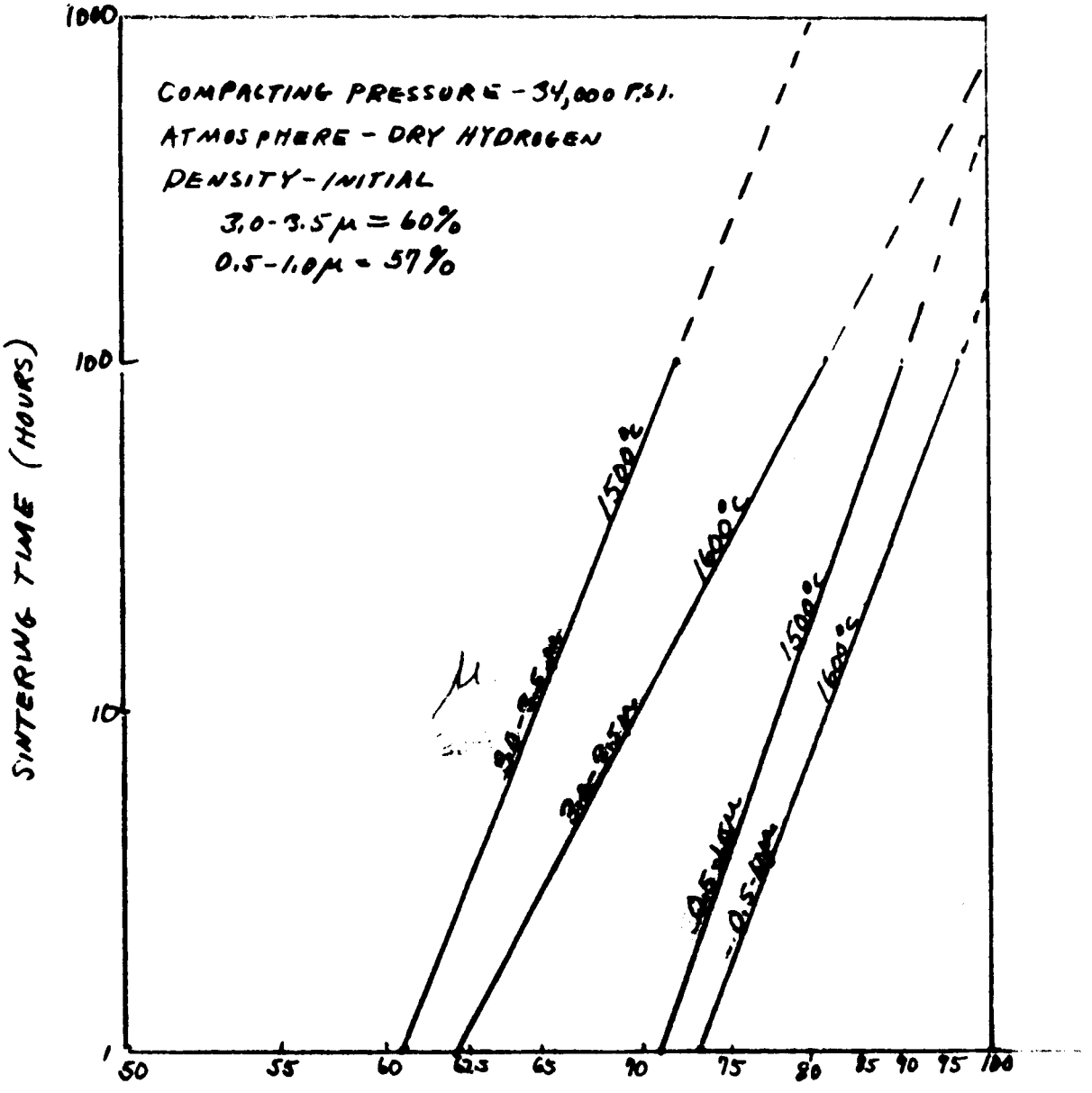

HUGHES RESEARCH LABORATORIES DATA

FIG 88 EFFECT OF PARTICLE SIZE AND DENSITY ON SINTERING TIME

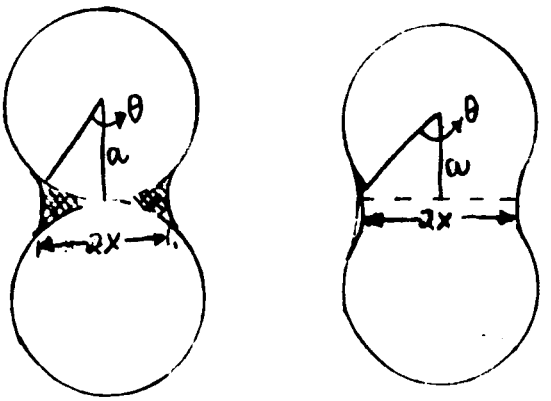

FIG 4. KUCZYNSKI'S MODEL FOR TWO STAGE SINTERING
SHOWING RELATIONSHIP BETWEEN
X - NECK WIDTH AND a - PARTICLE RADIUS,
θ IS THE ANGLE FORMED.

FIG 5 DUCKWORTHS MEASUREMENTS OF θ (CONTACT) ANGLE OF SINTERED SPHERES

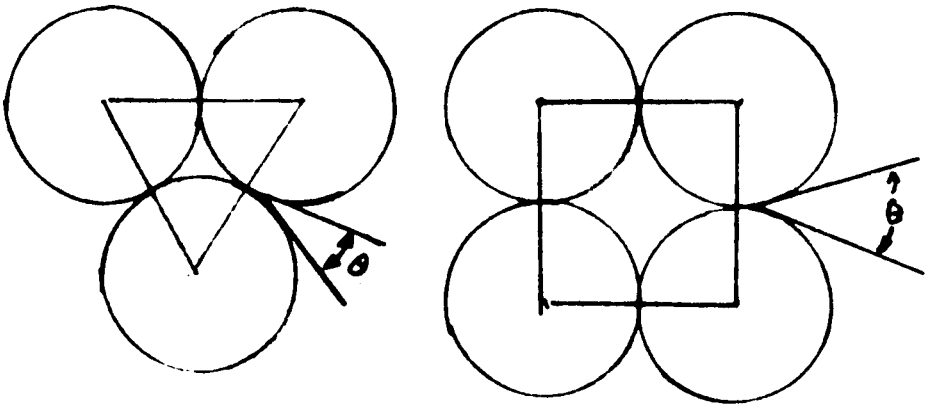

RHOMBIC PACKING CUBIC PACKING

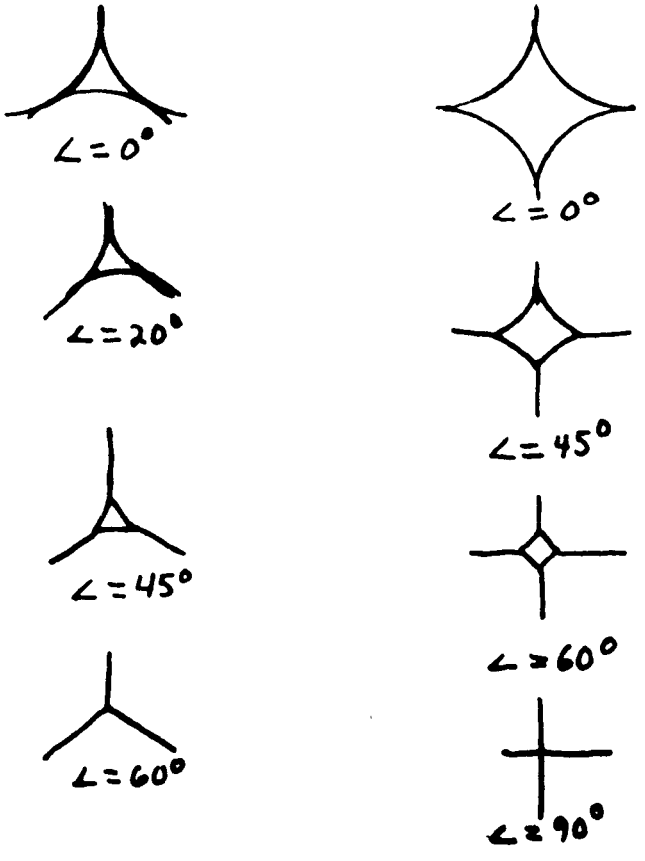

E 2130

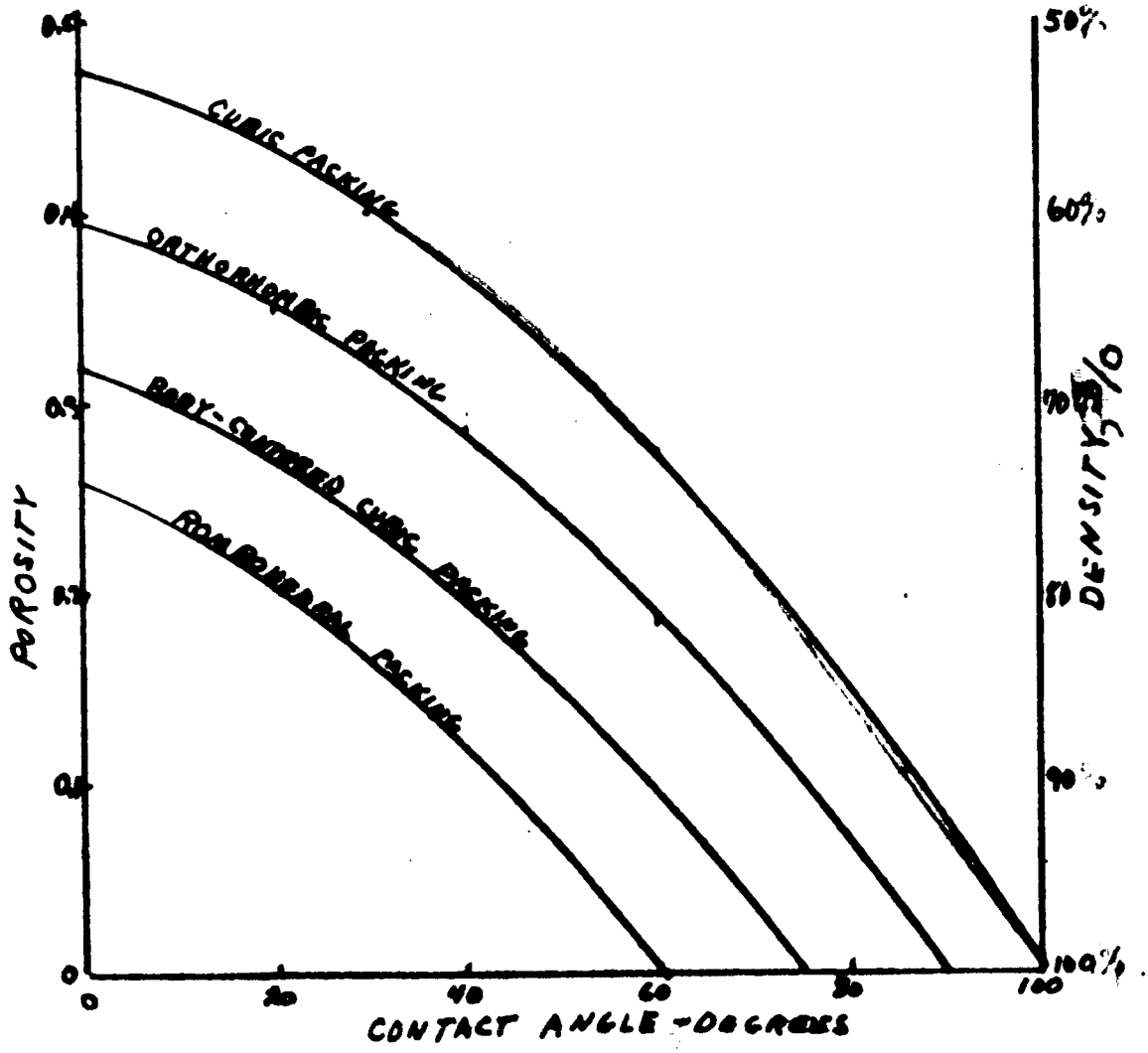

FIG 6 DUCKWORTHS RELATION-SHIP BETWEEN TYPE PACKING-TO THE VOLUME AVAILABLE BETWEEN SPHERES (POROSITY) AND DENSITY

E-2130

1) $x = \frac{\sqrt{3}}{2} \frac{a}{2}$

2) $x = \frac{\sqrt{3}}{2} \frac{a}{2}$

SURFACE DIFFUSION

$$\frac{x^7}{7} = \frac{\gamma \delta^4 V_a^2 D_s}{KT} \Delta t$$

VOLUME DIFFUSION

$$\frac{x^5}{5} = \frac{100 \gamma \delta^3 D_v}{KT} t$$

$$x^5 = \frac{100 \gamma \delta^3 D_v}{KT} t$$

$$5 \log x = \log t + \log \left(\frac{100 \gamma \delta^3 D_v}{KT} \right)$$

FIG 7 KUCZYNSKI'S SINTERING FORMULAR

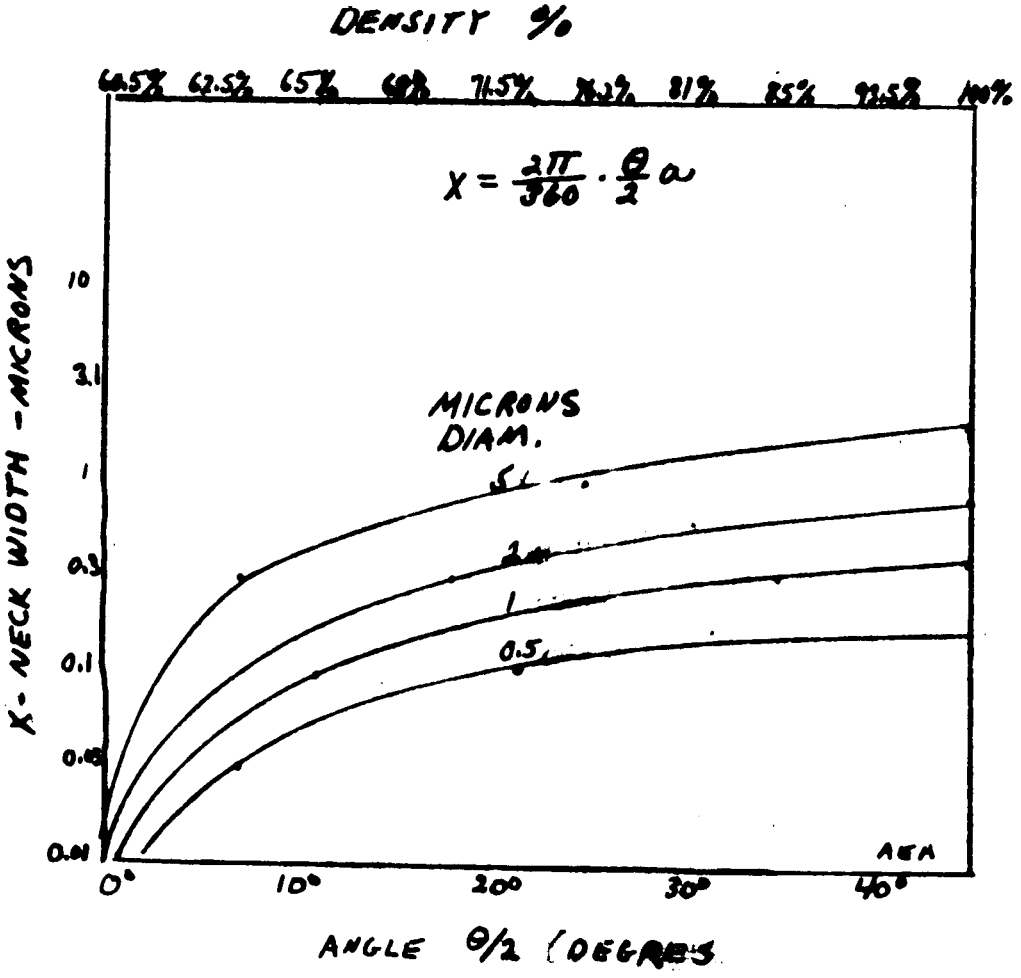

FIG 7A RELATIONSHIP BETWEEN θ(ANGLE) DENSITY - X(NECK WIDTH) AND PARTICLE DIAMETER FOR ARC METHOD.

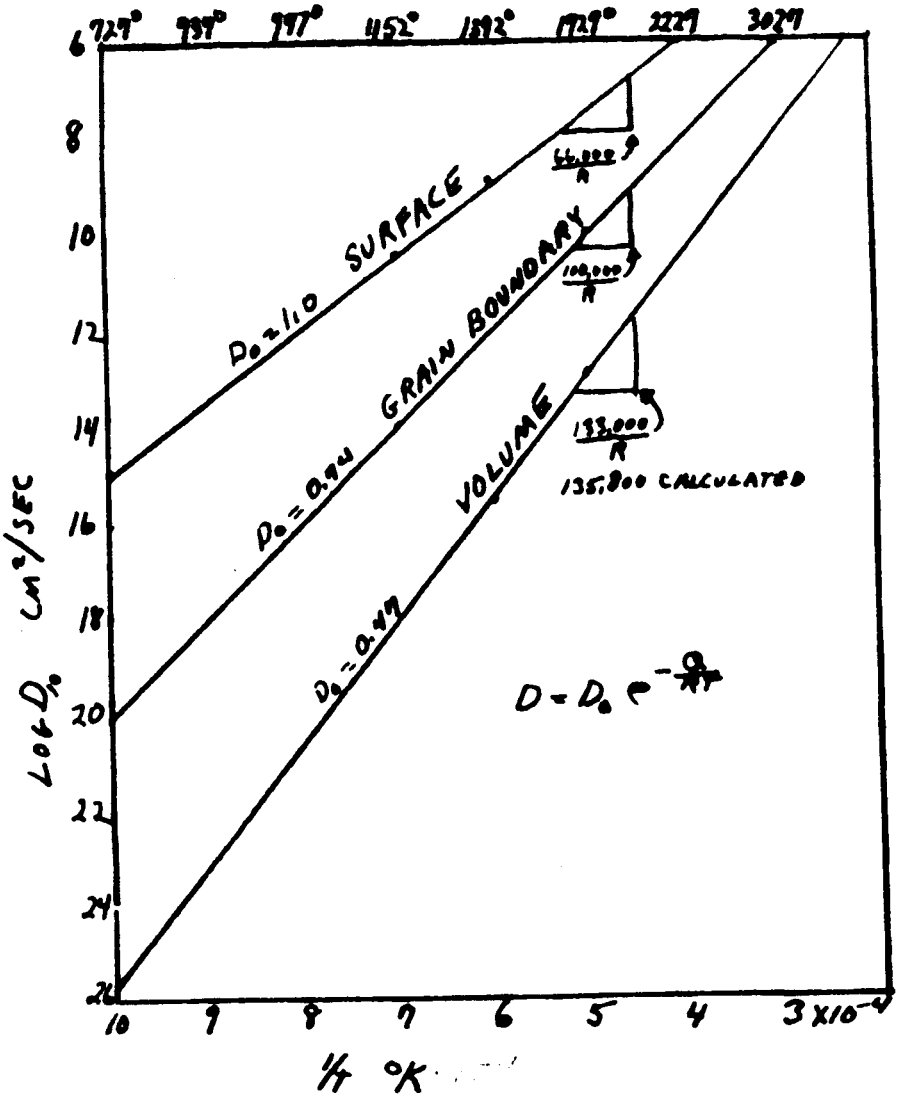

FIG 18 DIFFUSION OF THORIUM INTO TUNGSTEN - SLOPE EQUALS ENERGY OF ACTIVATION
LANGMUIR (10) & LECLAIRE (11)

E 2130

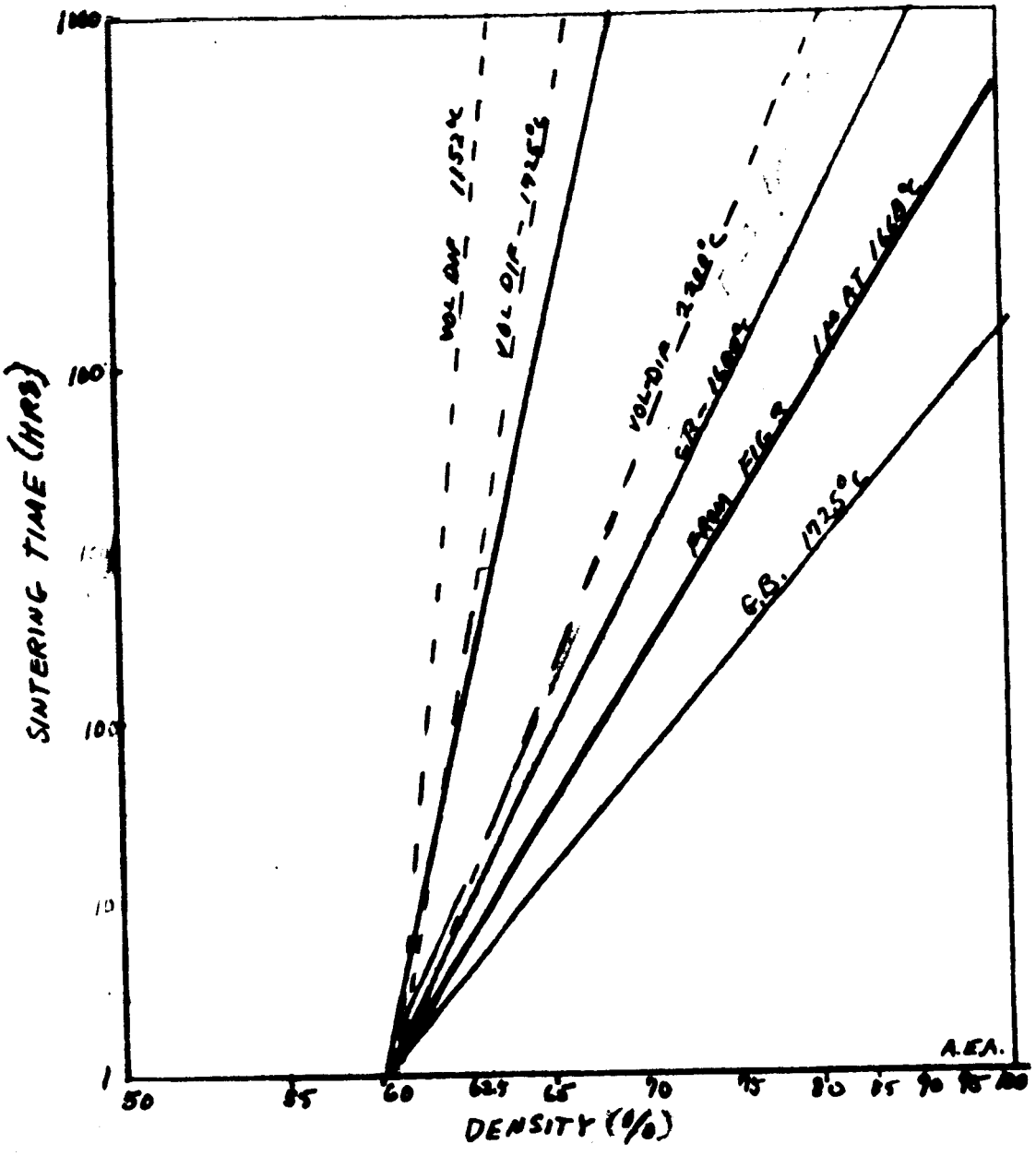

FIG 8. RESULTS OF CALCULATING NECK WIDTH BY MODIFIED THEORY FOR 2 MICRON DIAMETER PARTICLES

E-2130

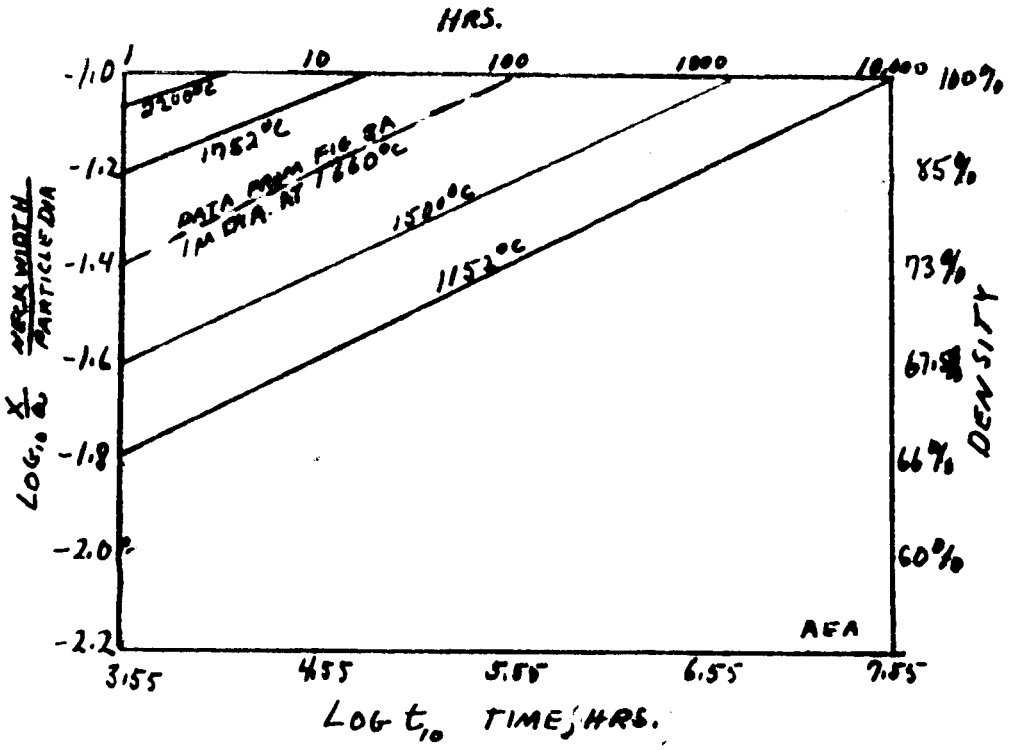

FIG-8A CALCULATED SINTERING RATE FOR GRAIN BOUNDARY DIFFUSION FOR 0.5 MICRON PARTICLES

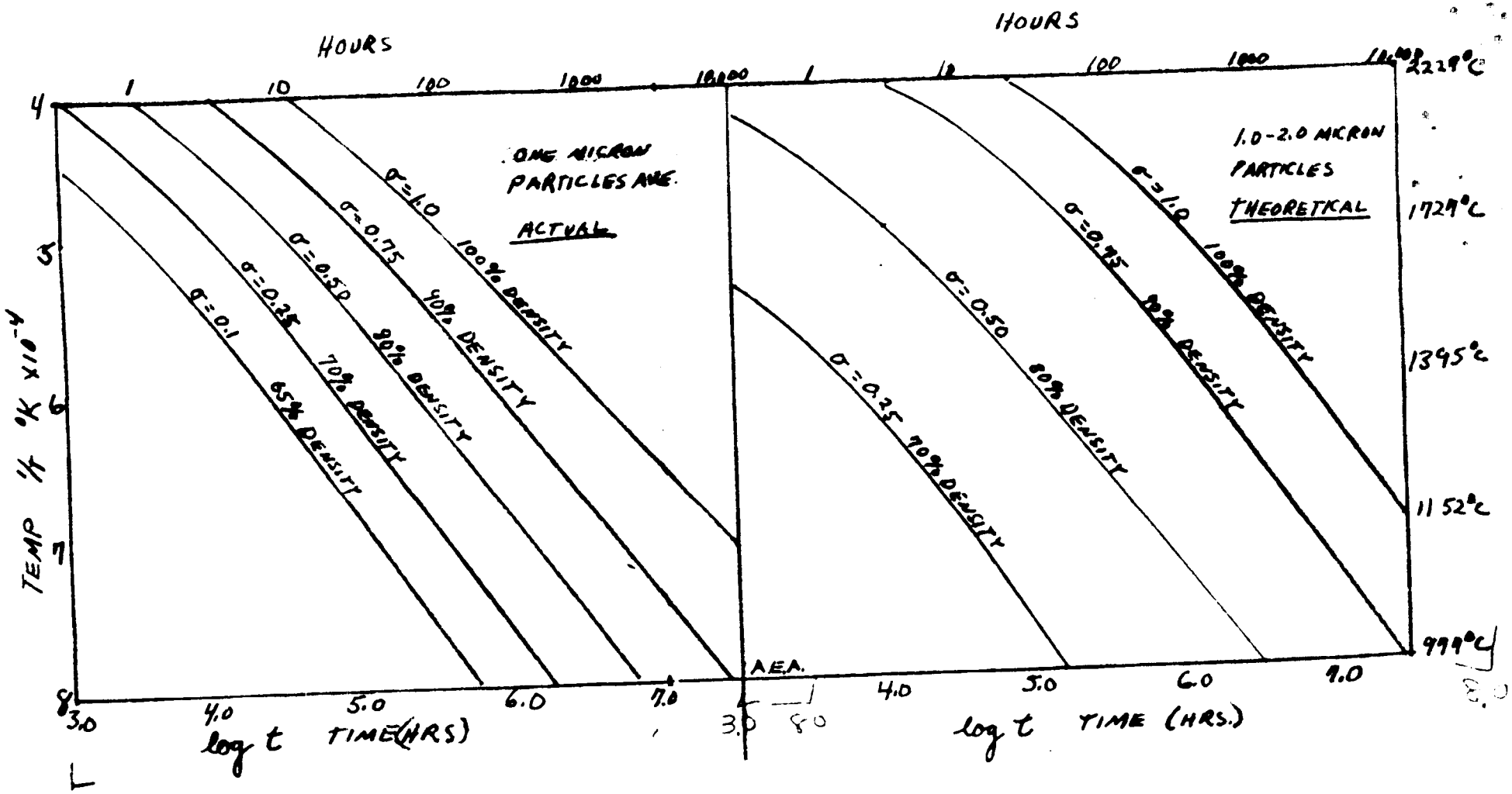

FIG 9 GRAIN BOUNDARY DIFFUSION RATES FOR TUNGSTEN SINTERING FROM JORDAN AND DUWEZ – TEMPERATURE AND TIME TO REACH HIGHER DENSITY

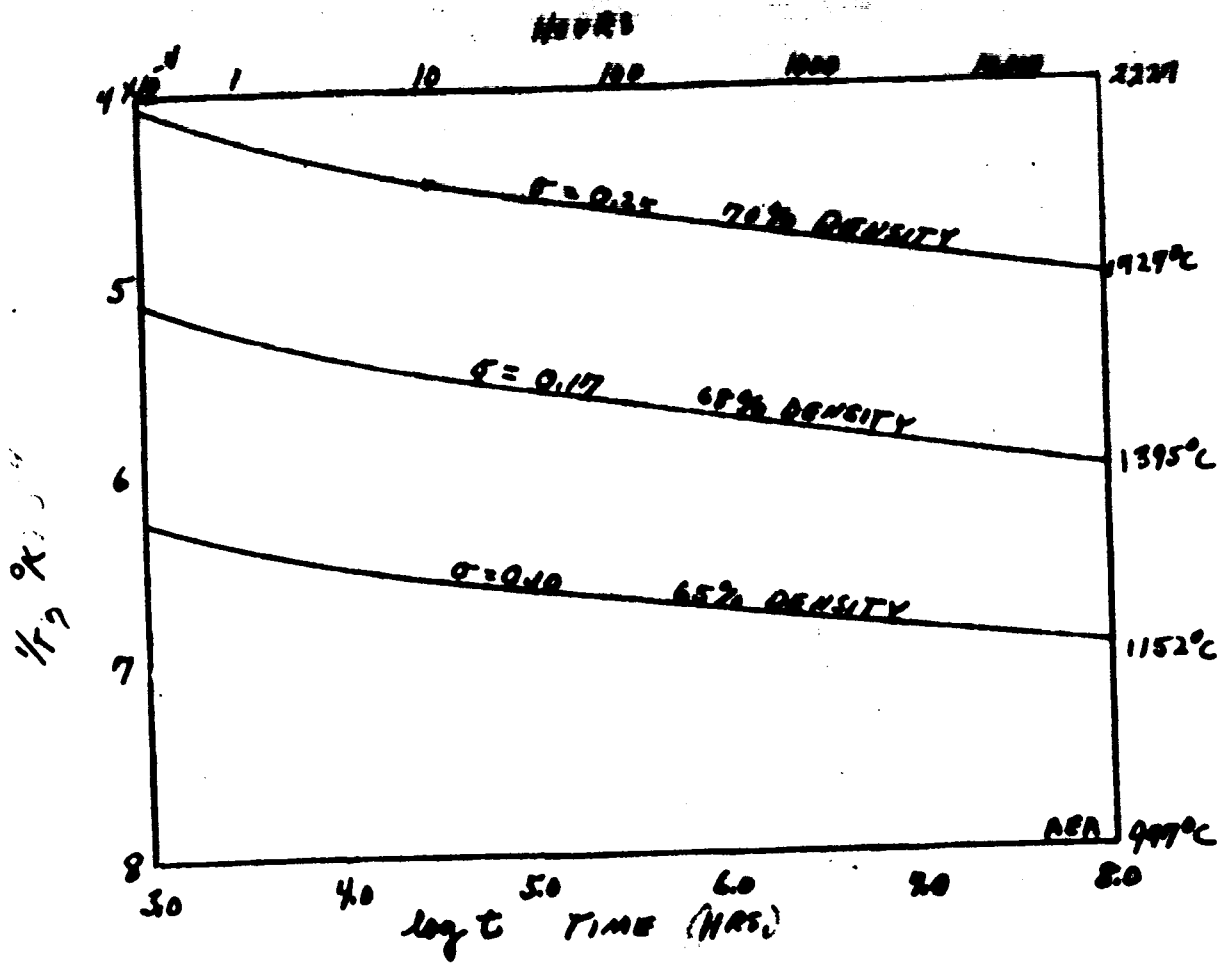

FIG 10 VOLUME DIFFUSION RATES FOR TUNGSTEN SINTERING. TEMPERATURE AND TIME TO REACH DENSITY FROM JORDAN & DUWEZ

E-2130

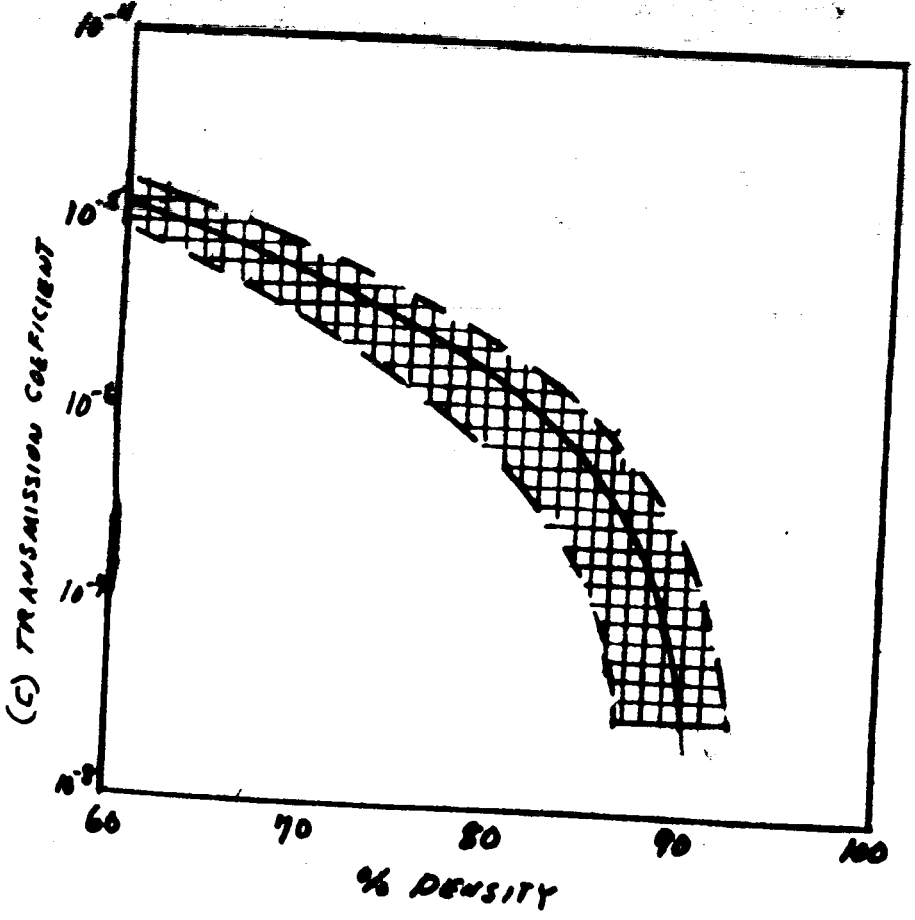

$C = \frac{\text{GAS DISPATURE RATE}}{\text{GAS ARRIVAL RATE}}$

$C = \frac{\sqrt{2\pi} \bar{E} V \delta P}{A \delta \bar{c} P}$

FOR N_2 AT 300°K

$C = \frac{8.122 \times 10^{-7} V \delta P_{mm}}{A \delta \bar{c}_{cm}}$

FIG 11 EFFECT OF DENSIFICATION ON THE TRANSMISSION COEFFICIENT ON ALL TYPES OF POROUS TUNGSTEN DISKS - SHOWN RESULTS OF RUTLEDGE AND RITNER. (17) DATA OF REYNOLDS AND SAUNDERS